
SEMI-PARAMETRIC MAKEUP TRANSFER VIA SEMANTIC-AWARE CORRESPONDENCE

A PREPRINT

 **Mingrui Zhu**

State Key Laboratory of Integrated Services Networks
Xidian University
Xi'an, China
mrzhu@xidian.edu.cn

 **Yun Yi**

State Key Laboratory of Integrated Services Networks
Xidian University
Xi'an, China
yuny220@163.com

 **Nannan Wang**

State Key Laboratory of Integrated Services Networks
Xidian University
Xi'an, China
nnwang@xidian.edu.cn

 **Xiaoyu Wang**

The Chinese University of Hong Kong (Shenzhen)
Shenzhen, China
fanghuaxue@gmail.com

 **Xinbo Gao**

Chongqing Key Laboratory of Image Cognition
Chongqing University of Posts and Telecommunications
Chongqing, China
gaoxb@cqupt.edu.cn

March 7, 2022

ABSTRACT

The large discrepancy between the source non-makeup image and the reference makeup image is one of the key challenges in makeup transfer. Conventional approaches for makeup transfer either learn disentangled representation or perform pixel-wise correspondence in a parametric way between two images. We argue that non-parametric techniques have a high potential for addressing the pose, expression, and occlusion discrepancies. To this end, this paper proposes a **Semi-parametric Makeup Transfer** (SpMT) method, which combines the reciprocal strengths of non-parametric and parametric mechanisms. The non-parametric component is a novel **Semantic-aware Correspondence** (SaC) module that explicitly reconstructs content representation with makeup representation under the strong constraint of component semantics. The reconstructed representation is desired to preserve the spatial and identity information of the source image while “wearing” the makeup of the reference image. The output image is synthesized via a parametric decoder that draws on the reconstructed representation. Extensive experiments demonstrate the superiority of our method in terms of visual quality, robustness, and flexibility. Code and pre-trained model are available at <https://github.com/AnonymScholar/SpMT>.

Keywords Makeup transfer · Semi-parametric · Semantic-aware correspondence · Generative adversarial networks

1 Introduction

Makeup transfer, aiming to apply cosmetics to a non-makeup face image by simulating a well-makeup one, has attracted tremendous interest and become an active topic in computer vision. Its applications can automatically improve users’ facial appearance with chosen makeup examples and therefore save a great deal of manual work.

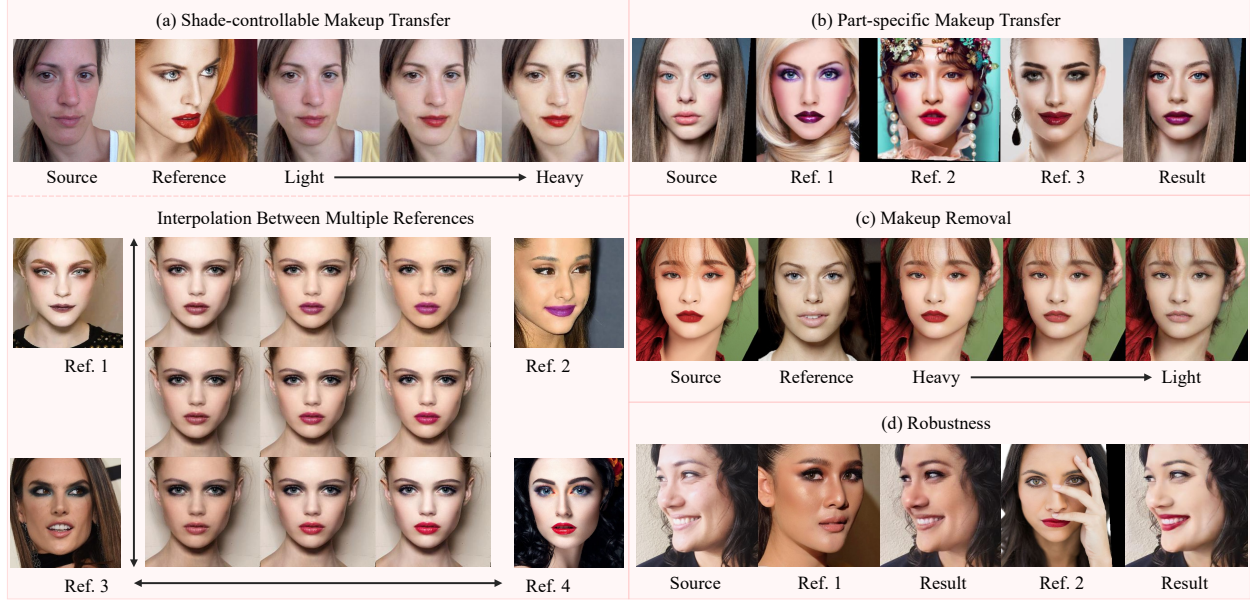


Figure 1: The proposed SpMT method combines the reciprocal strengths of non-parametric and parametric techniques and has natural advantages in flexibility and robustness. (a) Shade-controllable makeup transfer by interpolation between non-parametric reconstructed representations. (b) Part-specific makeup transfer by selecting different parts from different reconstructed representations. (c) Makeup removal that does not require a bi-directional mapping, all in one parametric decoder. (d) Robustness to environmental variants.

While early research endeavors [Tong et al., 2007] [Guo and Sim, 2009] [Li et al., 2015] mainly leverage image processing approaches to accomplish this task, significant progress, however, is driven by recent deep learning-based methods [Liu et al., 2016], the route of which has been much more prevalent since the booming of generative adversarial networks (GAN) [Goodfellow et al., 2014]. Inspired by CycleGAN [Zhu et al., 2017], a domain-level image-to-image translation model, PairedCycleGAN [Chang et al., 2018] and BeautyGAN [Li et al., 2018] tackle makeup transfer as an instance-level exemplar-based translation problem, which opens a new route for following studies. Recent advances in disentangled representation [Lee et al., 2018] also energize many works [Chen et al., 2019, Zhang et al., 2019a, Gu et al., 2019, Sun et al., 2020, Li et al., 2020] to learn the decomposition and recombination of makeup style representation and content representation. Currently, cutting-edge methods try to seek robust makeup transfer methods that can well adapt to the real-world scenario. Promising results have been reported in [Huang et al., 2020, Jiang et al., 2020, Deng et al., 2021, Wan et al., 2021, Lyu et al., 2021].

The aforementioned deep learning-based methods, despite demonstrating success, are all parametric models that represent the makeup procedure (*i.e.* mapping function) via their weights. They forsake the competency to draw on the material provided by examples in exchange for highly efficient end-to-end capability. One obvious defect is that they always fail to cover up freckles or blemishes on the faces. In addition, this may not consist of the practices of the makeup artist. Imagine the real makeup procedure: the makeup artist picks up a powder and applies it evenly on the face, or applies lipstick with a certain color number to the lips. In this procedure, facial makeup comes from real makeup tools. Imitating this process, makeup transfer may also take the material of the corresponding component directly from the reference makeup image and apply it to the source image in a non-parametric manner.

In this paper, we combine the reciprocal advantages of parametric and non-parametric techniques, and present a **Semi-parametric Makeup Transfer** (SpMT) approach. The non-parametric makeup procedure is achieved through a newly proposed **Semantic-aware Correspondence** (SaC) module. This module elegantly establishes a semantic-aware correspondence between the corresponding components of the source non-makeup image and the reference makeup image in their feature pyramids. Whether in the training or testing process, the module obtains raw materials from the reference image through the semantic-aware correspondence and reconstructs the representation of the source image. The advantages of the non-parametric SaC module lie in its robustness against environmental variants like pose, expression, or occlusion discrepancies and its flexibility on controllable makeup transfer (as shown in Figure 1). The reconstructed representation is then processed by an image reconstruction network that produces an after-makeup image as output in a parametric manner.

The contributions of this work are threefold:

- 1) A semi-parametric approach, which to our best knowledge, is the first to emphasize the potential of the non-parametric mechanism in the makeup transfer task.
- 2) A non-parametric SaC module accompanied with a cosmetic perceptual loss that establishes a semantic-aware correspondence between the non-makeup representation and makeup representation, which enables robustness and flexibility of the presented method.
- 3) Extensive experiments that demonstrate the superiority of the proposed method over state-of-the-arts and verify its capability to realize controllable and robust makeup transfer while yielding makeup images with satisfying quality.

2 Related Work

2.1 Makeup Transfer

Makeup transfer refers to such a kind of task that when given a pair of input images, transfer the specific makeup style from one of them (called reference image) to another (called source image) without destroying the face identity of the source input. It has been studied [Tong et al., 2007] [Guo and Sim, 2009] [Xu et al., 2013] [Li et al., 2015] for a decade before the ascendance of deep learning approaches. Rapid progress in deep convolutional neural networks, especially in generative adversarial networks, has inspired recent progress of makeup transfer. PairedCycleGAN [Chang et al., 2018] introduced an asymmetric makeup transfer framework based on CycleGAN [Zhu et al., 2017]. BeautyGAN [Li et al., 2018] utilized a dual input/output generative adversarial network and a pixel-level histogram loss on local regions to fulfill instance-level makeup transfer. Based on Glow architecture [Kingma and Dhariwal, 2018], BeautyGlow [Chen et al., 2019] decomposed the latent vectors into makeup vectors and facial identity vectors, and then invert the recombined vectors to the image domain. Gu et al. [2019] proposed LADN by incorporating local style discriminators, disentangling representation, and asymmetric loss functions into a cross-domain image translation network. Some studies [Zhang et al., 2019a] [Sun et al., 2020] [Li et al., 2020] also adopted the idea of disentangled representation learning. A recent line of studies [Huang et al., 2020] [Jiang et al., 2020] [Deng et al., 2021] [Wan et al., 2021] [Lyu et al., 2021] explored robust makeup transfer models that can well against the environmental variants. PSGAN [Jiang et al., 2020] introduced an attentive makeup morphing module based on an attention mechanism to realize partial, shade-controllable, and pose/expression robust makeup transfer. SCGAN [Deng et al., 2021] broke down the makeup transfer problem into a two-step extraction-assignment process and proposed a part-specific style encoder to map the makeup style into a component-wise style-code, which can eliminate the spatial misalignment problem. In this paper, we show that the proposed non-parametric SaC module, combined with the parametric decoder, also achieves excellent robustness and flexibility.

2.2 Semi-parametric Studies

The idea that combining the complementary strengths of parametric and non-parametric techniques has been cases in other research fields. Qi et al. [2018] proposed a semi-parametric model to synthesize a photographic image from semantic layouts. The non-parametric component of their model is a memory bank of training image segments which used as raw materials for drawing on the semantic layout. In the field of image style transfer, Liao et al. [2017] proposed a deep image analogy module that can find semantically-meaningful dense correspondences between two input images. Gu et al. [2018] proposed a feature reshuffle module that integrates global and local style losses which owns the advantages of both neural parametric and non-parametric methods. Sheng et al. [2018] and Zhang et al. [2019b] also adopted this idea and demonstrated its effectiveness. Zhang et al. [2020] proposed a CoCosNet to jointly learn the cross-domain correspondence and the image translation. Inspired by these studies, we address the robust makeup transfer task by proposing a semi-parametric model. The non-parametric component is inspired by [Chen and Schmidt, 2016], but we make a complete improvement by the proposed SaC module for the specific characteristic of makeup transfer (For a discussion on the differences between image style transfer and makeup transfer, please refer to [Li et al., 2018]).

3 Overview

Let $X = \{x_m \mid x_m \in X\}_{m=1, \dots, M}$ denote the examples sampled from the non-makeup image distribution \mathcal{P}_X and $Y = \{y_n \mid y_n \in Y\}_{n=1, \dots, N}$ denote the examples sampled from the makeup image distribution \mathcal{P}_Y . For the task of makeup transfer, we aim to generate an after-makeup image \hat{x} given a source non-makeup image x and a reference makeup image y . That is, learning the mapping function: $\hat{x} = \mathcal{G}(x, y)$. The generated image \hat{x} is desired to conform to the identity as x while resembling the makeup style of the reference image y .

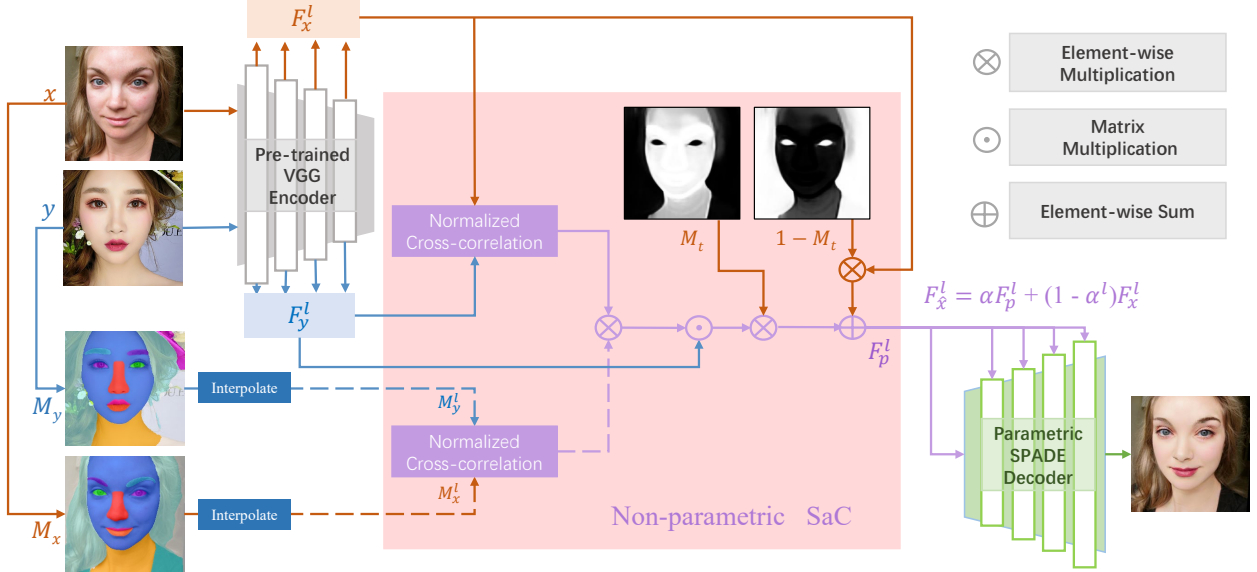


Figure 2: The illustration of the SpMT framework. Pre-trained VGG-19 is used to encode the input images into multi-scale (l denotes the scale number, $l = 1, 2, 3, 4$) deep representations. Then, the proposed SaC module reconstructs the pseudo representation in a non-parametric manner. The output image is synthesized via a parametric image reconstruction network that draws on the reconstructed representation. SpMT combines the reciprocal strengths of non-parametric and parametric mechanisms

Deep learning-based models typically represent the mapping function $\hat{x} = \mathcal{G}(x, y)$ via neural architectures with learnable weights, which belong to parametric models. Considering the advantage of non-parametric techniques for addressing the pose, expression, and occlusion discrepancies, we integrate the non-parametric module and parametric module in an end-to-end semi-parametric framework.

The pipeline of SpMT is shown in Figure 2. We utilize the pre-trained VGG-19 [Simonyan and Zisserman, 2014] to encode the source image x and the reference image y into their deep representations F_x^l and F_y^l , where l is the number of VGG-19 layers. Note that the parameters of the VGG-19 are frozen and will not change during training. Then, the proposed SaC module reconstructs pseudo-representation F_x^l given F_x^l and F_y^l in a non-parametric way. The reconstructed representation is desired to preserve the spatial distribution of F_x^l and the cosmetic style of F_y^l . Unlike existing approaches that learn the disentanglement between content and style, the SaC directly takes raw materials from F_y^l to decorate F_x^l , just like the makeup procedure performed by makeup artists. Note that the proposed SaC relies on facial mask M_x^l of the source image and facial mask M_y^l of the reference image that provides component semantics. SaC introduces semantic information into correspondence in a simple yet elegant way. The reconstructed representation F_x^l is used as input to a parametric image reconstruction network. This network synthesizes the final output image \hat{x} .

4 Semantic-aware Correspondence

Recent advances in attention mechanism [Wang et al., 2018] bring an efficient way to compute the response at a position as a weighted sum of the features at all positions, which establishes a dense pixel-wise correspondence between two matrices. However, the computational complexity on the spatial scale limits that it can only be calculated on the deep representations of small spatial size (generally the deep representations at the bottleneck). Actually, [Chen and Schmidt, 2016] provides another mechanism with the same effect but a different mean. Formally, let $\Psi(\cdot)$ denote the list of all local patches extracted from the deep representation. Each neural patch is indexed as $\Psi_i(\cdot)$ of the size $c \times k \times k$, where c is the number of channels and k is the spatial size of the patch. For each neural patch $\Psi_i(F_x^l)$, best matching patch $\Psi_{NN(i)}(F_y^l)$ can be found using normalized cross-correlation(NCC) over all N_y example patches in $\Psi(F_y^l)$:

$$NCC_{i,j}^l(F_x^l, F_y^l) = \frac{\Psi_i(F_x^l) \odot \Psi_j(F_y^l)}{|\Psi_i(F_x^l)| \odot |\Psi_j(F_y^l)|}, \quad (1)$$

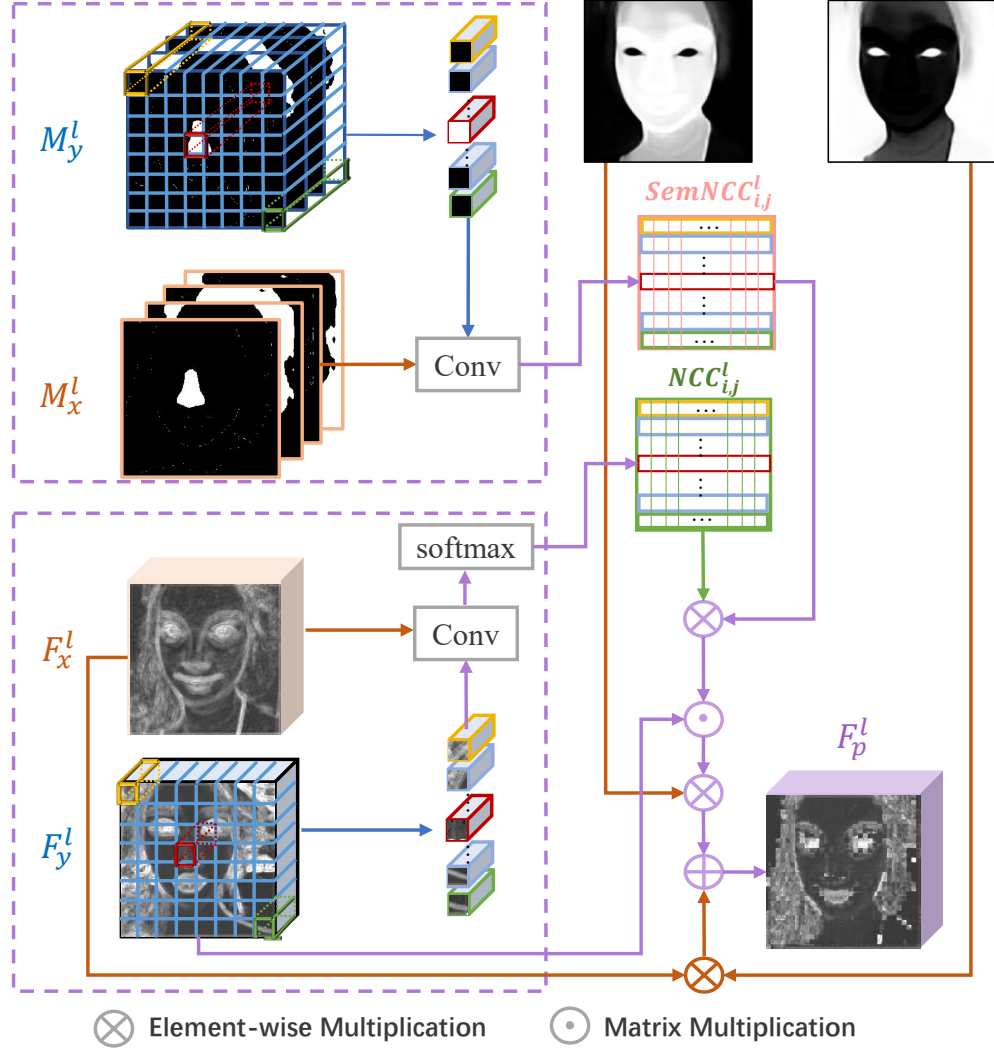


Figure 3: The illustration of the SaC module. SaC computes two types of normalized cross-correlation: the normalized cross-correlation computed on deep representations, and the normalized cross-correlation computed on facial semantics (as shown in the dashed box above). By performing element-wise multiplication between them, we can obtain the semantic-aware correspondence, which is capable of reconstructing F_p^l with makeup style patches only in the same semantic component

$$NN^l(i) := \arg \max_{j \in \{1, \dots, N_y\}} NCC_{i,j}^l(F_x^l, F_y^l). \quad (2)$$

This process is actually done by executing convolution operation on $\Psi(F_c^l)$ with custom convolution kernels $\Psi_i(F_y^l)$ and computing the max response, all in a feed-forward convolutional layer. When the spatial size of the patch is set to 1 and computing the softmax instead of the max response, this module has the same function as the pixel-wise correspondence in the attention mechanism:

$$\Psi_i(F_p^l) = \sum_j \text{softmax } NCC_{i,j}^l(F_x^l, F_y^l) \odot \Psi_j(F_y^l). \quad (3)$$

This module breaks the restriction that the correspondence can only be established at the pixel level, so it can be applied to deep representation with a larger spatial size by using a large patch size.

However, this module is far from enough for makeup transfer. Since the correspondence suggests the matched reference patches strictly similar to the source patches, the reconstructed representation $\Psi_i(F_p^l)$ will be highly biased towards the

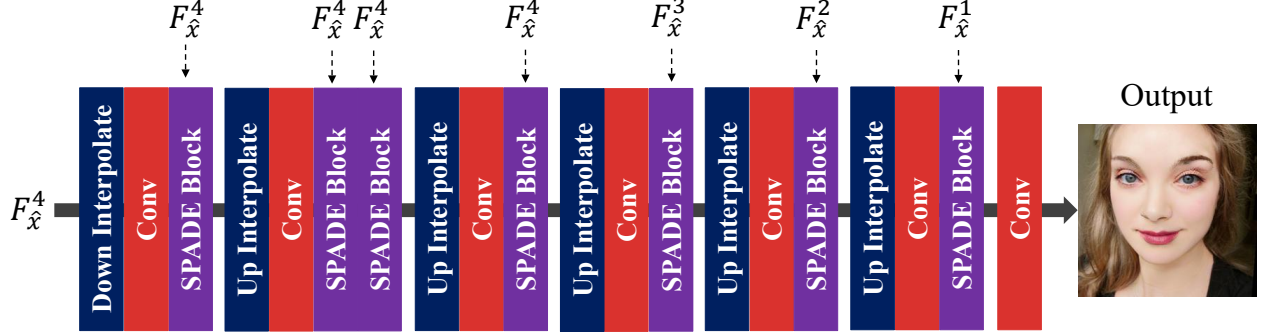


Figure 4: The architecture of the SPADE decoder.

source representation F_x^l and only a limited portion of cosmetic patterns are transferred to $\Psi_i(F_p^l)$, especially when F_x^l and F_y^l are significantly discrepant from each other. The effect on the reconstructed image is that the makeup style of the reference image has been washed out (as shown in Figure 5). In particular, in the makeup transfer task, makeup style (e.g. foundation, lipsticks, eye shadows) is more delicate and elaborate, which is closely related to local components. The global correspondence will destroy such local cosmetic patterns.

Therefore, we present the SaC module that establishes correspondence at the semantic component level. The illustration of the SaC module is shown in Figure 3. In addition to the normalized cross-correlation computed on deep representations of the source image and the reference image (as shown in the dashed box below), we define a normalized cross-correlation on their facial semantics (as shown in the dashed box above):

$$SemNCC_{i,j}^l(M_x^l, M_y^l) = \frac{\Psi_i(M_x^l) \odot \Psi_j(M_y^l)}{|\Psi_i(M_x^l)| \odot |\Psi_j(M_y^l)|}. \quad (4)$$

Note that M_x^l and M_y^l both have multiple channels. Each channel corresponds to one component (e.g. skin, lips, eyes). Each value in all channels is specified as 0 or 1, indicating that this position does not belong to or belongs to a specific component respectively. For example, a vector $[0, 1, 0, \dots, 0]$ of a spatial position indicates that this position belongs to the facial skin. Therefore, the response (i.e. dot product) of the vectors in two positions with the same semantic will be 1 and the response of the vectors in two positions with different semantics will be 0. By performing element-wise multiplication between $NCC_{i,j}^l$ and $SemNCC_{i,j}^l$, we can obtain the semantic-aware correspondence, which is capable of reconstructing $\Psi_i(F_p^l)$ with makeup style patches only in the same semantic component:

$$\begin{aligned} \Psi_i(F_p^l) &= \sum_j \text{softmax } NCC_{i,j}^l(F_x^l, F_y^l) \\ &\otimes SemNCC_{i,j}^l(M_x^l, M_y^l) \odot \Psi_j(F_y^l). \end{aligned} \quad (5)$$

By stitching patches of $\Psi_i(F_p^l)$ together, F_p^l is obtained. In the makeup transfer task, we only need to transfer the makeup of some specific components, so we can replace the parts in the reconstructed representation F_p^l that do not need to be transferred with the source representation through mask M_t :

$$F_p^l = M_t \otimes F_p^l + (1 - M_t) \otimes F_x^l. \quad (6)$$

M_t is a binary mask, where all positions with a value of 1 constitute components that need makeup transfer and positions with a value of 0 constitute components that do not need makeup transfer.

In practice, we find that directly using F_p^l will produce slight artifacts on a few generated images. Therefore, before inputting the reconstructed representation F_p^l into the parametric image reconstruction network, we add different proportions of content features to F_p^l on different scales to get a more stable performance:

$$F_{\hat{x}}^l = SaC(x, y) = \alpha^l F_p^l + (1 - \alpha^l) F_x^l, \quad (7)$$

where $F_{\hat{x}}^l$ denotes the final reconstructed representation obtained via the SaC module $SaC(x, y)$.

Since the proposed SaC module works in a non-parametric manner and relies on facial masks to establish the semantic-aware correspondence, it can well against environmental variants like large pose, expression, and occlusion discrepancies. In addition, SaC can also achieve high flexibility like shade-controllable and part-specific by controlling the combination of $F_{\hat{x}}^l$ and F_x^l through facial masks and weights.

5 Image Reconstruction Network

5.1 SPADE Decoder

We require a feed-forward parametric model \mathcal{G} which takes as input the multi-scale reconstructed representation $F_{\hat{x}}^l$ to reconstruct the after-makeup output \hat{x} . To this end, we design an image reconstruction network that consists of several spatially-adaptive de-normalization (SPADE) [Park et al., 2019] blocks. Each scale of the reconstructed representation $F_{\hat{x}}^l$ is used as input of each SPADE block to learn the modulation parameters α^l and β^l . The produced α^l and β^l are multiplied and added to the normalized activation of the output of the previous layer element-wise. Formally, given the activation $F^l \in \mathfrak{R}^{c_l \times h_l \times w_l}$ before the l^{th} block, we inject the $F_{\hat{x}}^l$ through:

$$\alpha_{h_l, w_l}^l(F_{\hat{x}}^l) \times \frac{F_{c_l, h_l, w_l}^l - \mu_{h_l, w_l}^l}{\sigma_{h_l, w_l}^l} + \beta_{h_l, w_l}^l(F_{\hat{x}}^l). \quad (8)$$

The overall parametric reconstruction can be formulated as:

$$\hat{x} = \mathcal{G}(F_{\hat{x}}^l; \theta_{\mathcal{G}}), \quad (9)$$

where $\theta_{\mathcal{G}}$ denotes the learnable parameter.

The architecture of the SPADE decoder is shown in Figure 4. The reconstructed representation $F_{\hat{x}}^4$ at *Relu_4_1* is firstly down-interpolated and then gradually up-interpolated to reconstruct the output image. The image reconstruction network comprises 7 SPADE blocks. Each SPADE block is introduced to de-normalize the activations with learned parameters γ and β from a reconstructed representation $F_{\hat{x}}^l$. We use *bilinear* interpolation and *kernel* = 3×3 – *stride* = 1 – *padding* = 1 convolution in this architecture.

5.2 Loss Function

5.2.1 Adversarial Loss

We use the Least Squares GAN [Mao et al., 2017] to provide adversarial loss for the parametric SPADE decoder, which can help generate plausible natural-looking images with high perceptual quality. For the mapping function \mathcal{G} and its discriminator \mathcal{D} , we express the adversarial loss as:

$$\begin{aligned} \mathcal{L}_{adv} = & \mathbb{E}_{x, y}[(\mathcal{D}_Y(x, y))^2] \\ & + \mathbb{E}_{x, y}[(1 - \mathcal{D}_Y(x, \mathcal{G}(SaC(x, y))))^2]. \end{aligned} \quad (10)$$

5.2.2 Content Loss

Since some parts (*e.g.* teeth, hair, etc.) in the makeup transfer task do not need to be transferred, a content loss is introduced to keep the non-transferred parts unchanged:

$$\mathcal{L}_{con} = \mathbb{E}_{x, y}[\|(\mathcal{G}(SaC(x, y)) - x) \otimes (1 - M_t)\|_2]. \quad (11)$$

5.2.3 Cosmetic perceptual Loss

The reconstructed representation $F_{\hat{x}}^l$ by the proposed non-parametric SaC module can be further used as pseudo-ground-truth to guide the training of \mathcal{G} . Therefore, we propose a cosmetic perceptual loss to substitute the raw perceptual loss [Johnson et al., 2016] that is commonly used in existing methods. Let $\Phi^l(\cdot)$ denote the pyramid representation derived from the pre-trained VGG-19, the cosmetic perceptual loss is computed by:

$$\mathcal{L}_{cos} = \mathbb{E}_{x, y}[\sum_l \|\Phi^l(\mathcal{G}(SaC(x, y))) - F_{\hat{x}}^l\|_2]. \quad (12)$$

Since the reconstructed representation can preserve the spatial distribution of the source representation and the cosmetic style of the reference representation, this loss can force the generated image to preserve the spatial distribution of the source image and the cosmetic style of the reference image.

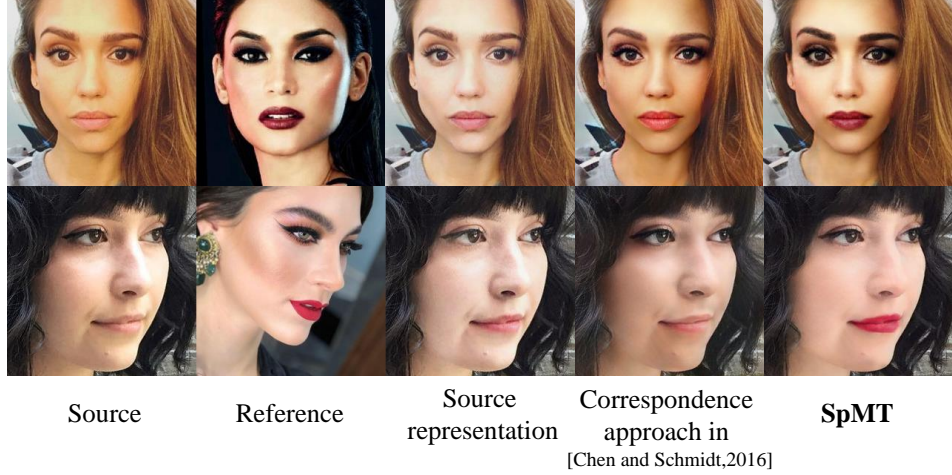


Figure 5: Ablation study of the proposed SaC module.

5.2.4 Style Loss

A certain proportion of global style loss can help improve the overall style of the output image, we use mean and variance of the representation in VGG-19 layers to model global style:

$$\begin{aligned} \mathcal{L}_{sty} = & \mathbb{E}_{x,y} \left[\sum_l \|\mu(\Phi^l(\mathcal{G}(SaC(x,y)))) - \mu(\Phi^l(y))\|_2 \right. \\ & \left. + \sum_l \|\sigma(\Phi^l(\mathcal{G}(SaC(x,y)))) - \sigma(\Phi^l(y))\|_2 \right]. \end{aligned} \quad (13)$$

5.2.5 Makeup Loss

We utilize the makeup loss proposed by [Li et al., 2018] to further guide the makeup style of lips, eye shadows, and face regions:

$$\mathcal{L}_{makeup} = \mathbb{E}_{x,y} [\mathcal{G}(SaC(x,y)) - HM(x,y)]_1, \quad (14)$$

where $HM(\cdot, \cdot)$ denotes the histogram matching in lips, eye shadows, and face regions and the output of $HM(x, y)$ has the makeup style of y while preserving the identity of x .

5.2.6 Total Loss

By combining the above losses, we can achieve our full loss:

$$\begin{aligned} \mathcal{L}_{total} = & \lambda_{adv} \mathcal{L}_{adv} + \lambda_{makeup} \mathcal{L}_{makeup} \\ & + \lambda_{cos} \mathcal{L}_{cos} + \lambda_{sty} \mathcal{L}_{sty} + \lambda_{con} \mathcal{L}_{con}, \end{aligned} \quad (15)$$

where λ_{adv} , λ_{makeup} , λ_{cos} , λ_{sty} , and λ_{con} are the weights to balance the multiple objectives.

6 Experiments

6.1 Experimental Settings

In this section, we first discuss the experimental settings. Then, we conduct an ablation study to quantify the contribution of different configurations to the overall effectiveness. Further, we evaluate the flexibility and robustness of the proposed model. Finally, we qualitatively and quantitatively compare our results with state-of-the-art methods.

6.1.1 Implementation details.

Feature activations extracted from *Relu_1_1*, *Relu_2_1*, *Relu_3_1* and *Relu_4_1* layers of the pre-trained VGG-19 [Simonyan and Zisserman, 2014] are used as deep representations of input images. To establish semantic-aware

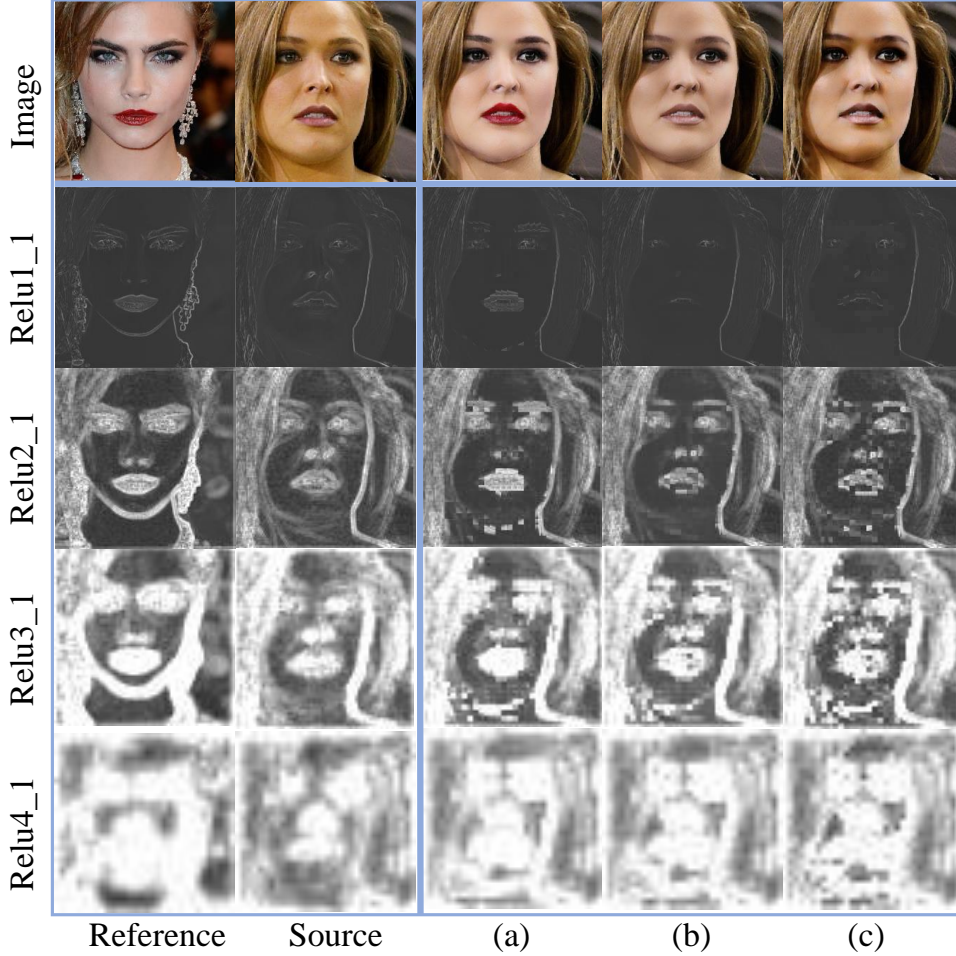


Figure 6: Reconstructed multi-scale features and transferred images with different correspondence methods. (a) The proposed semantic-aware correspondence. (b) Weighted correspondence. (c) Nearest patch correspondence [Chen and Schmidt, 2016]. To facilitate the comparison of generated makeup, we show the input reference image in the upper left corner.

correspondence, we use 8×8 patch size for $Relu_1_1$, 4×4 patch size for $Relu_2_1$, 2×2 patch size for $Relu_3_1$ and 1×1 patch size for $Relu_4_1$. The convolution stride for each layer is equal to the patch size so that there is no overlap between the extracted patches.

We set $\lambda_{adv} = 1$, $\lambda_{makeup} = 1$, $\lambda_{cos} = 5$, $\lambda_{sty} = 10$, $\lambda_{con} = 100$. RMSProp optimizer with default parameters is utilized for optimization. The learning rate is fixed at 0.0002 and the batch size is set to 1. We scale the size of the input images to 256×256 and normalize the pixel value to the interval $[-1, 1]$ before putting them into the model. To acquire facial masks, we use the face parsing model provided in [zllrunning], which is trained on the CelebAMask-HQ database [Lee et al., 2020].

6.1.2 Dataset

Our model was trained on the Makeup Transfer (MT) dataset [Li et al., 2018] which contains 3834 images. It consists of 2719 makeup images and 1115 non-makeup images including variations in race, poses, expression, and background clutter. We use the same setting as Li et al. [2018] that randomly select 100 non-makeup images and 250 makeup images for testing. The rest of the images are used for training.

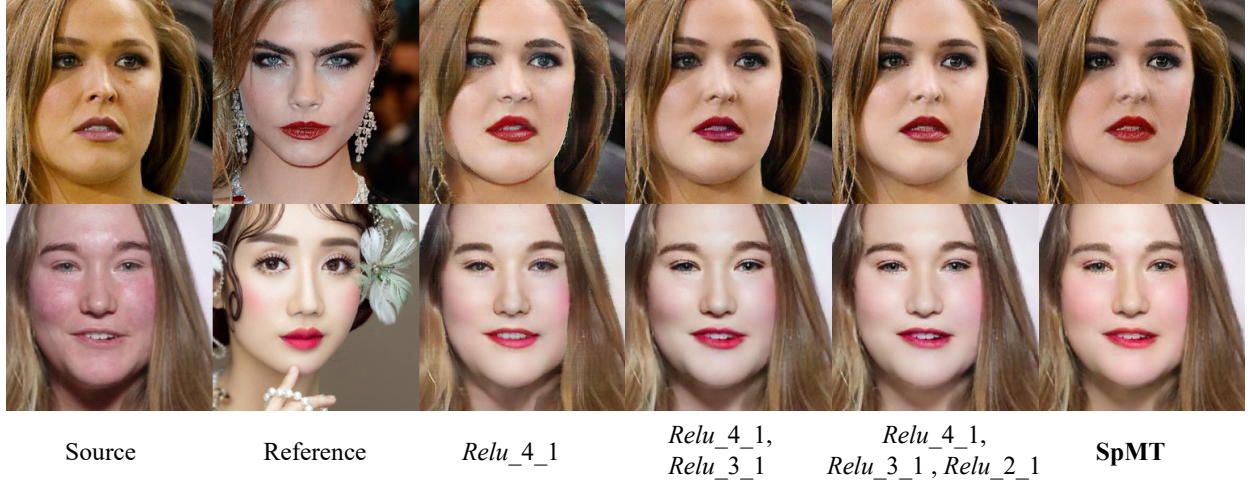


Figure 7: Ablation study about the effect of different scales of the reconstructed representation on the final performance.



Figure 8: Ablation study of cosmetic perceptual loss.

6.2 Ablation Study

Four contributions conduce to the overall efficacy.

6.2.1 Non-parametric semantic-aware correspondence

To verify the superiority of the SaC module, we replace it with the other two modules to observe the change of performance. Figure 5 shows the results. When directly using the source representation instead of the reconstructed representation as to the input of the SPADE decoder, the generated image has almost no makeup style of the reference image. But its overall style is changing towards the reference image with the help of the parametric decoder. When using the correspondence approach provided by [Chen and Schmidt, 2016] instead of the SaC module, the makeup effect of the generated image will also be reduced. The global correspondence will wash away the local cosmetic patterns when the source image and the reference image are significantly discrepant from each other. The proposed SaC module establishes correspondence at the semantic component level to explicitly retain cosmetic patterns, thus producing the best results.

Figure 9: Ablation study of α^l .

Figure 6 visualizes the reconstructed multi-scale features and transferred images with different correspondence modules. As we can see, compared with the other two correspondence modules, features reconstructed by the proposed SaC module can better preserve the component content and transfer more reasonable makeup style.

6.2.2 Multi-scale

The effect of different scales of the reconstructed representation on the final performance is shown in Figure 7. Using only the reconstructed representation of *Relu_4_1* will cause some structural distortion on the generated image. Add *Relu_3_1* and *Relu_2_1* can alleviate this problem and present synthetic image with reasonable structure. However, when zoomed in, the problem that they lack reasonable style patterns in the hair, eye shadow, and foundation area will be exposed. SpMT that uses all layers of reconstructed representations can achieve the best results.

Figure 6 further presents the visualization results of the reconstructed representation of different scales. Reconstructed features of *Relu_4_1* and *Relu_3_1* contain the main structure and identity information of the image. Reconstructed

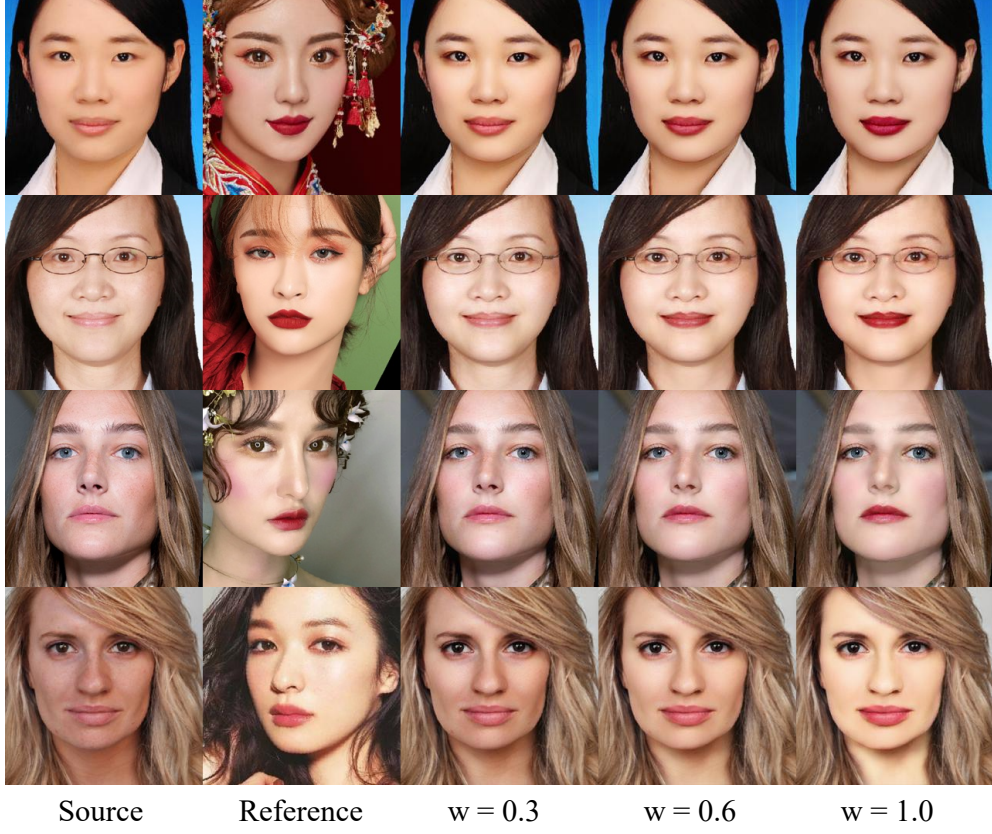


Figure 10: Results of interpolated makeup styles. Adjusting the shade of makeup.

features of *Relu_2_1* and *Relu_1_1* possess more texture information of the image. Therefore, by introducing the multi-scale mechanism, the proposed method also has the nice property that synthesizing the image from coarse-to-fine.

6.2.3 Cosmetic perceptual loss

To verify the efficacy of the cosmetic perceptual loss, we replace this loss with vanilla perceptual loss and observe the performance change. Figure 8 shows the results. As we can see, compared with the vanilla perceptual loss, the cosmetic perceptual loss can transfer a more delicate and more consistent makeup style from the reference image to the source image.

6.2.4 Setting of α^l

As mentioned in Sec. 4, we do not directly use the reconstructed representation F_p^l as input to the SPADE decoder because it will produce slight artifacts on a few generated images. Therefore, we add different proportions of content features to F_p^l on different scales (as shown in Eq. 7) to get the final reconstructed representation F_x^l with more stable performance. Note that the α^l for each layer has a different value. We empirically set $\alpha^4 = 0.1$, $\alpha^3 = 0.2$, $\alpha^2 = 0.4$, and $\alpha^1 = 1$ to gradually reduce the proportion of content representation. The input of the first four blocks are reconstructed representations ($\alpha^4 = 0.1$) at *Relu_4_1*. The input of the 5th block is the reconstructed representation ($\alpha^3 = 0.2$) at *Relu_3_1*. The input of the 6th block is the reconstructed representation ($\alpha^2 = 0.4$) at *Relu_2_1*. The input of the 7th block is the reconstructed representation ($\alpha^1 = 1$) at *Relu_1_1*. The ablation results are shown in Figure 9. When α^l is set to 1, which means directly using F_p^l as input to the SPADE decoder, some artifacts will be produced on the output images. By fusing content representation in a certain proportion, the SpMT shows more stable performance.

6.3 Flexibility and Robustness

Since SpMT possesses a non-parametric module SaC, it has natural advantages in controllability and robustness.

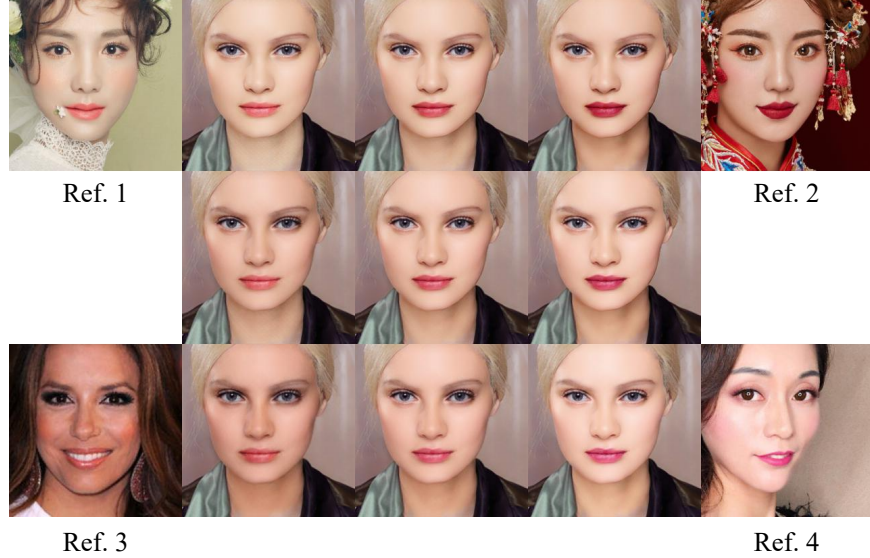


Figure 11: Results of interpolated makeup styles. Interpolation between four references.

6.3.1 Shade-controllable transfer

Shade-controllable transfer can be realized simply by interpolating the combined coefficient ($w \in [0, 1]$) of content representation and reconstructed representation:

$$R_s = wF_{\hat{x}}^l + (1 - w)F_x^l \quad (16)$$

By inputting the re-combined representation R_s (with w from 0 to 1) into the learned parametric SPADE decoder, we can gradually change the makeup style from the source image to the reference image.

SpMT also supports fusing the makeup styles from multiple reference images with a linear interpolation:

$$R_s = w_1F_{\hat{x}-ref1}^l + w_2F_{\hat{x}-ref2}^l + \dots + w_kF_{\hat{x}-refk}^l \quad (17)$$

where $w_1 + w_2 + \dots + w_k = 1$. By changing the value of w_k , we can fuse multiple makeup styles from different reference images.

Figure 1 (a) shows the interpolated makeup transfer results and the makeup transfer results produced by mixing four reference images, which demonstrates the superb flexibility of SpMT. Figure 10 and Figure 11 present more examples of shade-controllable makeup transfer. Our method can adjust the shade of makeup and interpolation between multiple references.

6.3.2 Part-specific transfer

Since SpMT uses facial masks to distinguish semantic components and provide semantic constraints, it can easily perform part-specific makeup transfer by choosing any specific part from any reference image. For example, if we want to transfer the makeup styles of the lip, eye-shadow, and foundation from *Ref1*, *Ref2*, and *Ref3* respectively, we can manipulate their reconstructed representation by:

$$R_s = M_l \otimes F_{\hat{x}-Ref1}^l + M_e \otimes F_{\hat{x}-Ref2}^l + M_f \otimes F_{\hat{x}-Ref3}^l + (1 - M_t) \otimes F_x^l \quad (18)$$

where M_t is a binary mask indicating where a transfer is required, M_l , M_e , and M_f are binary masks indicating the lip, eye, and skin components. The result presented in Figure 1 (b) successfully transferred the lip color, eye shadow, and foundation style from Ref.1, Ref.2, and Ref.3 respectively. Figure 12 shows some examples of part-specific makeup transfer. Our method can transfer makeup styles from different parts of different references to a single output image.

6.3.3 Makeup removal

Thanks to the powerful SaC module, the proposed SpMT method can achieve makeup removal by directly taking the non-makeup image as the reference image and the makeup one as the source image. SaC can reconstruct the



Figure 12: Results of part-specific makeup transfer. Transfer makeup styles from different parts of different references.

non-makeup representation while keeping the identity of the makeup image. Note that SpMT does not require a bi-directional mapping as existing methods and performs image reconstruction using one SPADE decoder. Figure 1 (c) and Figure 13 show makeup removal results from heavy to light.

6.3.4 Robustness

As mentioned before, SpMT has excellent robustness to the environmental variants owed to the advantage of the SaC module. Results presented in Figure 1 (d) and Figure 15 demonstrate this superiority.

6.4 Comparison with Prior Arts

To validate the efficacy of the proposed method, we compare it with two general domain transfer methods CycleGAN [Zhu et al., 2017] and DIA [Liao et al., 2017] as well as six state-of-the-art makeup transfer methods PairedCycleGAN [Chang et al., 2018], BeautyGAN [Li et al., 2018], BeautyGlow [Chen et al., 2019], LADN [Gu et al., 2019], PSGAN [Jiang et al., 2020] and SCGAN [Deng et al., 2021]. Since the code of BeautyGlow and PairedCycleGAN are not available, we directly copy the results of BeautyGlow and PairedCycleGAN from their papers following the strategy used in BeautyGlow. The results of other methods are obtained by running their official code with the default configuration.

6.4.1 Qualitative comparison

Figure 14 shows the qualitative comparison of SpMT with other state-of-the-art methods on normal faces without large pose, expression, and occlusion variants. Since DIA performs patch matching globally and has no semantic control, its results fail to maintain the content of components that do not need makeup transfer and fail to transfer a correct makeup style. Without the reference image, CycleGAN can not perform instance-level makeup transfer that imitates the specified makeup style. Results of PairedCycleGAN and BeautyGlow also have incorrect makeup styles that are inconsistent with the reference image, such as the color of the foundation. Severe artifacts affect the overall appearance



Figure 13: Results of makeup removal.



Figure 14: Qualitative comparison with existing methods on normal faces without a large pose, expression, and occlusion variants.

of the results produced by LADN. BeautyGAN, PSGAN, and SCGAN perform well on these examples but still suffer from some minor defects.

To verify the robustness against the environmental variants such as pose, expression, and occlusion discrepancies, we further conduct a comparison with BeautyGAN, PSGAN, and SCGAN on some more challenging examples. The results are shown in Figure 15. As shown in the first row, when the makeup style of the input reference image is very thick, the results of the other three existing methods are affected, with uneven cosmetic, artifacts or significant noise. If there is occlusion on the face of the reference image, the result obtained by PSGAN appears obvious shadow at the corresponding position (the forehead of the face shown in the third row), which affects the appearance of the image. When the expression of the input source image is exaggerated as shown in the fourth row, cosmetic patterns of the lips appeared inside the mouth of the image generated by BeautyGAN, which damages the structure of the component. Another defect of these three methods is that the foundations of their results are not well imitating the reference images.

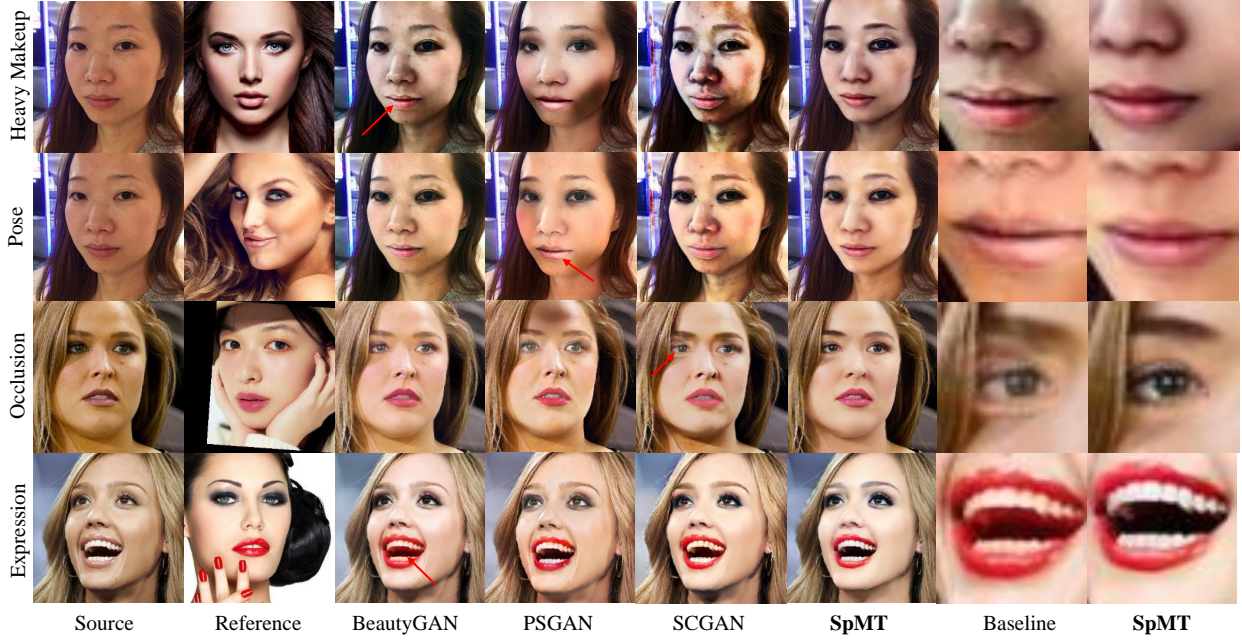


Figure 15: Qualitative comparison with existing methods on faces with a large makeup style, pose, occlusion, and expression variants. The last two columns are the enlarged view of the area marked by the red arrow in baseline and the enlarged view of the corresponding part of SpMT.

Method	BeautyGAN	PSGAN	SCGAN	SpMT
Western	155.1	156.7	154.5	141.3
vFG	175.7	162.8	159.0	156.4
vHX	140.6	131.8	136.7	119.2

Table 1: The experiment results of makeup style transferring

The wrinkles and blemishes on the face are not well covered up (see the last two column of the first row for example), which is an unwanted result when people are beautifying themselves with cosmetics. Compared with cutting-edge methods, SpMT can produce better results with a more uniform and exquisite cosmetic style and fewer artifacts. For more results, please refer to Figure 16.

6.4.2 Quantitative comparison

To compare the results of our method with the existing methods more objectively, we further conduct quantitative experiments.

For a particular makeup style, the images generated by a better makeup transfer algorithm should have a more similar distribution with its input reference images. Therefore, we calculated the Fréchet Inception Distance (FID) [Heusel et al., 2017] between the synthetic images and the reference images to measure the effect of makeup style transfer. Each row of Table 1 shows the FID score for each method on one kind of makeup style. Every score was calculated using 300 images generated by randomly selected 10 non-makeup images and 30 with-makeup images. Results show that our model achieves the lowest FID score in the transfer of three makeup styles, which proves that our method can get results that more consistent with the makeup style of the reference image.

After makeup transfer, the content and structure information of the input image should not be changed. So we use Structural Similarity Index Metric (SSIM) [Wang et al., 2004] to evaluate the degree of content maintenance. A higher score corresponds to better content preservation. From the results shown in Table 2, we can see that the SSIM score of our method is higher than other methods, which demonstrates the superiority of our method in maintaining the structure of the input source image.

Method	BeautyGAN	PSGAN	SCGAN	SpMT
SSIM↑	0.87	0.80	0.81	0.89

Table 2: The experiment results of identity preserving

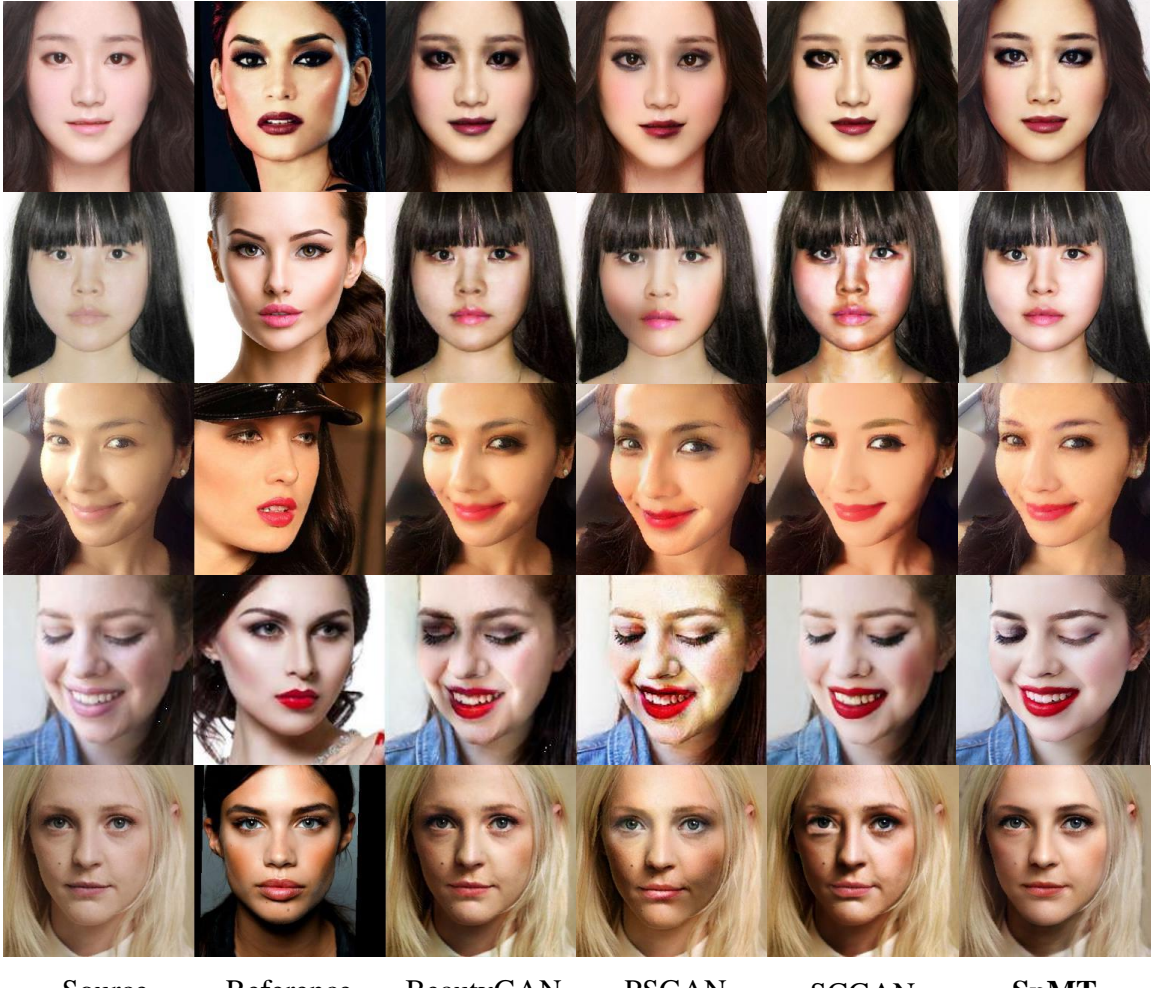


Figure 16: Additional examples of qualitative comparisons with existing methods

6.4.3 User study

We conducted a user study to evaluate our algorithm against 3 state-of-the-art makeup transfer methods: BeautyGAN, PSGAN, and SCGAN. It consists of two parts. In the first part, we randomly selected 20 non-makeup images and 20 makeup images that are well-aligned. Link of the first part: <https://www.wenjuan.com/s/UZBZJvJrWR/#>. In the second part, we randomly selected 20 non-makeup images and 20 makeup images which are faces with a large pose, expression, and occlusion variants. Link of the second part: <https://www.wenjuan.com/s/aMRRJf2/#>. After performing makeup transfer between these images, we obtained 400 after-makeup images for each method in each part. During the test, 15 groups of results in part 1 and 15 groups of results in part 2 were randomly presented to the participant. For each group, the placement order of the 4 synthetic images was shuffled and participants were asked to vote for their favorite result. Finally, we collected 1400 votes from 35 participants and calculated the percentage of votes for each method. The results are shown in Figure 17. SpMT obtains the highest ratio of votes on both two parts.

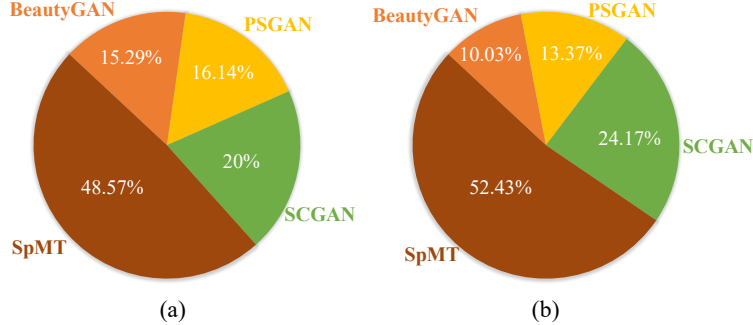


Figure 17: User study results. (a) Ratio of votes on the results of well-aligned images. (b) Ratio of votes on the results of images with a large pose, expression, and occlusion variants.

7 Conclusion

In this paper, we propose a semi-parametric approach for makeup transfer. Unlike existing methods that represent the mapping function from non-makeup images to makeup ones totally via parametric neural networks, the proposed method has a novel non-parametric semantic-aware correspondence module that directly gets raw materials from the reference image representation and decorates the source image representation. By combining the reciprocal strengths of parametric and non-parametric modules, the proposed approach achieves a great degree of flexibility and robustness. SpMT has a limitation that the non-parametric part is somewhat computational-expensive. It takes about 1 second to generate an image using a single Nvidia 3090 GPU. Properly reducing the number of layers of reconstruction representations can alleviate this problem. We will also explore more efficient techniques in the future.

References

Wai-Shun Tong, Chi-Keung Tang, Michael S Brown, and Ying-Qing Xu. Example-based cosmetic transfer. In *15th Pacific Conference on Computer Graphics and Applications (PG'07)*, pages 211–218. IEEE, 2007.

Dong Guo and Terence Sim. Digital face makeup by example. In *2009 IEEE Conference on Computer Vision and Pattern Recognition*, pages 73–79. IEEE, 2009.

Chen Li, Kun Zhou, and Stephen Lin. Simulating makeup through physics-based manipulation of intrinsic image layers. In *Proceedings of the IEEE Conference on Computer Vision and Pattern Recognition*, pages 4621–4629, 2015.

Si Liu, Xinyu Ou, Ruihe Qian, Wei Wang, and Xiaochun Cao. Makeup like a superstar: Deep localized makeup transfer network. *arXiv preprint arXiv:1604.07102*, 2016.

Ian Goodfellow, Jean Pouget-Abadie, Mehdi Mirza, Bing Xu, David Warde-Farley, Sherjil Ozair, Aaron Courville, and Yoshua Bengio. Generative adversarial nets. *Advances in neural information processing systems*, 27, 2014.

Jun-Yan Zhu, Taesung Park, Phillip Isola, and Alexei A Efros. Unpaired image-to-image translation using cycle-consistent adversarial networks. In *Proceedings of the IEEE international conference on computer vision*, pages 2223–2232, 2017.

Huiwen Chang, Jingwan Lu, Fisher Yu, and Adam Finkelstein. Pairedcyclegan: Asymmetric style transfer for applying and removing makeup. In *Proceedings of the IEEE conference on computer vision and pattern recognition*, pages 40–48, 2018.

Tingting Li, Ruihe Qian, Chao Dong, Si Liu, Qiong Yan, Wenwu Zhu, and Liang Lin. Beautygan: Instance-level facial makeup transfer with deep generative adversarial network. In *Proceedings of the 26th ACM international conference on Multimedia*, pages 645–653, 2018.

Hsin-Ying Lee, Hung-Yu Tseng, Jia-Bin Huang, Maneesh Singh, and Ming-Hsuan Yang. Diverse image-to-image translation via disentangled representations. In *Proceedings of the European conference on computer vision (ECCV)*, pages 35–51, 2018.

Hung-Jen Chen, Ka-Ming Hui, Szu-Yu Wang, Li-Wu Tsao, Hong-Han Shuai, and Wen-Huang Cheng. Beautyglow: On-demand makeup transfer framework with reversible generative network. In *Proceedings of the IEEE/CVF Conference on Computer Vision and Pattern Recognition*, pages 10042–10050, 2019.

Honglun Zhang, Wenqing Chen, Hao He, and Yaohui Jin. Disentangled makeup transfer with generative adversarial network. *arXiv preprint arXiv:1907.01144*, 2019a.

Qiao Gu, Guanzhi Wang, Mang Tik Chiu, Yu-Wing Tai, and Chi-Keung Tang. Ladn: Local adversarial disentangling network for facial makeup and de-makeup. In *Proceedings of the IEEE/CVF International Conference on Computer Vision*, pages 10481–10490, 2019.

Zhaoyang Sun, Feng Liu, Wen Liu, Shengwu Xiong, and Wenxuan Liu. Local facial makeup transfer via disentangled representation. In *Proceedings of the Asian Conference on Computer Vision*, 2020.

Yi Li, Huaibo Huang, Jie Cao, Ran He, and Tieniu Tan. Disentangled representation learning of makeup portraits in the wild. *International Journal of Computer Vision*, 128(8):2166–2184, 2020.

Zhiyun Huang, Zhedong Zheng, Chenggang Yan, Hongtao Xie, Yaoqi Sun, Jianzhong Wang, and Jiyong Zhang. Real-world automatic makeup via identity preservation makeup net. In *IJCAI*, pages 652–658, 2020.

Wentao Jiang, Si Liu, Chen Gao, Jie Cao, Ran He, Jia Shi Feng, and Shuicheng Yan. Psgan: Pose and expression robust spatial-aware gan for customizable makeup transfer. In *Proceedings of the IEEE/CVF Conference on Computer Vision and Pattern Recognition*, pages 5194–5202, 2020.

Han Deng, Chu Han, Hongmin Cai, Guoqiang Han, and Shengfeng He. Spatially-invariant style-codes controlled makeup transfer. In *Proceedings of the IEEE/CVF Conference on Computer Vision and Pattern Recognition*, pages 6549–6557, 2021.

Zhaoyi Wan, Haoran Chen, Jielei Zhang, Wentao Jiang, Cong Yao, and Jiebo Luo. Facial attribute transformers for precise and robust makeup transfer. *arXiv preprint arXiv:2104.02894*, 2021.

Yueming Lyu, Jing Dong, Bo Peng, Wei Wang, and Tieniu Tan. Sogan: 3d-aware shadow and occlusion robust gan for makeup transfer. *arXiv preprint arXiv:2104.10567*, 2021.

Lin Xu, Yangzhou Du, and Yimin Zhang. An automatic framework for example-based virtual makeup. In *2013 IEEE International Conference on Image Processing*, pages 3206–3210. IEEE, 2013.

Diederik P Kingma and Prafulla Dhariwal. Glow: Generative flow with invertible 1x1 convolutions. *arXiv preprint arXiv:1807.03039*, 2018.

Xiaojian Qi, Qifeng Chen, Jiaya Jia, and Vladlen Koltun. Semi-parametric image synthesis. In *Proceedings of the IEEE Conference on Computer Vision and Pattern Recognition*, pages 8808–8816, 2018.

Jing Liao, Yuan Yao, Lu Yuan, Gang Hua, and Sing Bing Kang. Visual attribute transfer through deep image analogy. *arXiv preprint arXiv:1705.01088*, 2017.

Shuyang Gu, Congliang Chen, Jing Liao, and Lu Yuan. Arbitrary style transfer with deep feature reshuffle. In *Proceedings of the IEEE Conference on Computer Vision and Pattern Recognition*, pages 8222–8231, 2018.

Lu Sheng, Ziyi Lin, Jing Shao, and Xiaogang Wang. Avatar-net: Multi-scale zero-shot style transfer by feature decoration. In *Proceedings of the IEEE Conference on Computer Vision and Pattern Recognition*, pages 8242–8250, 2018.

Yulun Zhang, Chen Fang, Yilin Wang, Zhaowen Wang, Zhe Lin, Yun Fu, and Jimei Yang. Multimodal style transfer via graph cuts. In *Proceedings of the IEEE/CVF International Conference on Computer Vision*, pages 5943–5951, 2019b.

Pan Zhang, Bo Zhang, Dong Chen, Lu Yuan, and Fang Wen. Cross-domain correspondence learning for exemplar-based image translation. In *Proceedings of the IEEE/CVF Conference on Computer Vision and Pattern Recognition*, pages 5143–5153, 2020.

Tian Qi Chen and Mark Schmidt. Fast patch-based style transfer of arbitrary style. *arXiv preprint arXiv:1612.04337*, 2016.

Karen Simonyan and Andrew Zisserman. Very deep convolutional networks for large-scale image recognition. *arXiv preprint arXiv:1409.1556*, 2014.

Xiaolong Wang, Ross Girshick, Abhinav Gupta, and Kaiming He. Non-local neural networks. In *Proceedings of the IEEE conference on computer vision and pattern recognition*, pages 7794–7803, 2018.

Taesung Park, Ming-Yu Liu, Ting-Chun Wang, and Jun-Yan Zhu. Semantic image synthesis with spatially-adaptive normalization. In *Proceedings of the IEEE/CVF Conference on Computer Vision and Pattern Recognition*, pages 2337–2346, 2019.

Xudong Mao, Qing Li, Haoran Xie, Raymond YK Lau, Zhen Wang, and Stephen Paul Smolley. Least squares generative adversarial networks. In *Proceedings of the IEEE international conference on computer vision*, pages 2794–2802, 2017.

Justin Johnson, Alexandre Alahi, and Li Fei-Fei. Perceptual losses for real-time style transfer and super-resolution. In *European conference on computer vision*, pages 694–711. Springer, 2016.

zllrunning. zllrunning/face-parsing.pytorch. <https://github.com/zllrunning/face-parsing.PyTorch>. URL <https://github.com/zllrunning/face-parsing.PyTorch>.

Cheng-Han Lee, Ziwei Liu, Lingyun Wu, and Ping Luo. Maskgan: Towards diverse and interactive facial image manipulation. In *Proceedings of the IEEE/CVF Conference on Computer Vision and Pattern Recognition*, pages 5549–5558, 2020.

M. Heusel, H. Ramsauer, T. Unterthiner, B. Nessler, and S. Hochreiter. Gans trained by a two time-scale update rule converge to a local nash equilibrium. In *Conference and Workshop on Neural Information Processing Systems*, 2017.

Zhou Wang, Alan C Bovik, Hamid R Sheikh, and Eero P Simoncelli. Image quality assessment: from error visibility to structural similarity. *IEEE Transactions on Image Processing*, 13(4):600–612, 2004.